Increasing Cone-beam projection usage by temporal fitting

Mark Lyksborg, Mads Fogtmann Hansen and Rasmus Larsen

Informatics and Mathematical Modeling, Technical University of Denmark
Richard Petersens Plads, Building 321, DK-2800 Kgs. Lyngby, Denmark
{mlyk, rl, mfh}@imm.dtu.dk

1 Introduction

A Cone-beam CT system can be used to image the lung region. The system records 2D projections which will allow 3D reconstruction however a reconstruction based on all projections will lead to a blurred reconstruction in regions were respiratory motion occur. To avoid this the projections are typically positioned on the breathing cycle using the Amsterdam shroud method [7] or some external measurement device. Measurement with similar respiratory positions are grouped as belonging to the same respiration phase. This preprocessing is known as phase binning and allows for the reconstruction of each sorted data set. The common method of choice for reconstructing the 3D volume is the Feldkamp-Davis-Kress algorithm [2], however this method suffers from serious artefacts when the sample number of projections is too low which can happen due to phase binning. Iterative methods based on solving the forward projection problem [1] are known to be more robust in these situations.

We study how the lower projection limits of an iterative method can be pushed even further by modelling a temporal relation between the respiratory phases. Although phase binned data is assumed the approach will work with raw measurements. It has been suggested in [8] to circumvent the Cone beam CT(CBCT) reconstruction by utilizing an ordinary planning CT instead and learning its deformation from the CBCT projection data. The main problem with this approach is that pathological changes can cause problems. Alternatively as suggested in [6] prior knowledge of the lung deformation estimated from the planning CT could be used to include all projections into the reconstruction. It has also been attempted to estimate both the motion and 3D volume simultaneously in [4]. Problems with motion estimation are ill-posed leading to suboptimal motion which in return affects the reconstruction. By directly including time into the image representation the effect of suboptimal motion fields are avoided and we are still capable of using phase neighbour projections.

The 4D image model is fitted by solving a statistical cost function based on Poisons assumptions using an L-BFGS-B optimizer [5]. It will be demonstrated on a phantom data set that the information gained from a 4D model leads to smaller reconstruction errors than a 3D iterative reconstruction based on phase binned data.

2 Cone-beam Geometry

A Cone-Beam system emits radiation from a point source towards a 2D detector plate which measures the total attenuation caused by the object/patient. The source and detector rotate simultaneously around the object while acquiring a sequence of projection images and each projection measurement is assumed to measure the integrated attenuation loss along an x-ray line L_i from the source towards the ith sensor(pixel) within the detector. A model for the expected value of the P_i sensor value is

$$E[P_i] = c_i \cdot e^{-\int_{L_i(\varphi)} \mu(\vec{x})\partial\vec{x}} + r_i, \tag{1}$$

and the goal is to determine μ such that the expected value match the true value. The c_i parameter models hardware variability of each sensor and can be determined from air calibration scans. The r_i parameter represents unaccounted for noise components such as photon scattering.

3 Method

3.1 The image model

For the purpose of reconstructing a choice of image representation has to be made. In tomographic reconstruction a popular choice is to let the image be represented as a weighted combination of the compactly supported basis functions positioned throughout the reconstruction region. Our choice is to use a spline model with cubic basis functions. Since we are looking for to utilize as much projection data as possible for any phase reconstruction, the spline is made 4 dimensional, $\mu : \Re^4 \rightarrow \Re^1$

$$\mu(\vec{x}) = \sum_i \sum_j \sum_k \sum_l b_i(x) b_j(y) b_k(z) b_l(t) w_{ijkl}. \tag{2}$$

This naturally increase the splines evaluation complexity but yield the effect that each reconstructed phase volume will be impacted by projections from its nearest neighbour phases.

3.2 Likelihood cost function

To fit the parameters w of the image model an optimality criteria is required. Under the assumption that the sensor measurements are Poison distributed a maximum likelihood cost function [1] can be formulated as

$$C = \sum_i p_i \cdot ln(E[P_i]) - E[P_i] \tag{3}$$

Inserting Eq. (1) and (2) into Eq. (3) and differentiating the cost function with respect to image model parameters, one obtains the gradient required for large scale optimization.

3.3 Image model boundaries

The usage of a spline based image model allows/demands a user specified choice on the behaviour of the spline at domain boundaries. An often used choice in medical imaging is the zero boundary condition forcing the model to zero at domain boundaries. This will be the choice for the 3 spatial dimensions. For the temporal phase dimension a more suitable choice is the periodic boundary condition. This corresponds to an assumption of breathing being periodic.

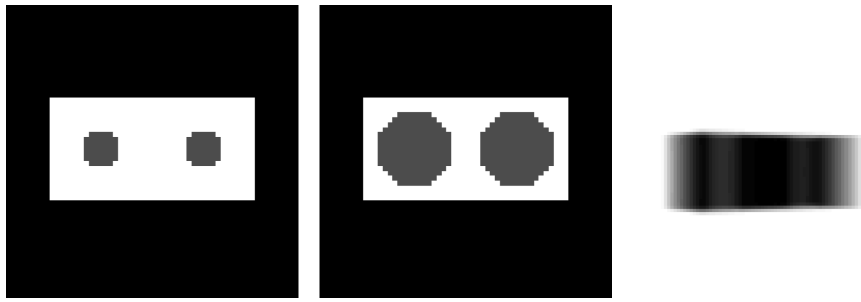

(a) Phase 1 (b) Phase 5 (c) Projection-Phase 1

Figure 1: (a)-(b) Shows slices from phantom data at phase 1 and phase 5. (c) Shows an example of a simulated projection at phase 1.

Table 1: Shows the results of reconstructing 5 phases, using cross correlation to compare with original data.

n projs.	Phase 1		Phase 2		Phase 3		Phase 4		Phase 5	
	4D	3D	4D	3D	4D	3D	4D	3D	4D	3D
5	0.9674	0.8675	0.9684	0.9600	0.9594	0.8892	0.9562	0.9268	0.9434	0.9243
10	0.9768	0.9754	0.9762	0.9684	0.9718	0.9692	0.9552	0.8843	0.9430	0.9399
20	0.9819	0.9802	0.9789	0.9751	0.9747	0.9719	0.9749	0.9688	0.9729	0.9713

3.4 Optimization

To fit the image model parameters of Eq. (2) a Newton minimization routine is used requiring the maximization problem of Eq. (3) to be turned into a minimization problem which is done by negation of the function. The L-BFGS-B optimizer [5] is used. By requiring $w_{ijkl} > 0$ the image attenuation values are forced to obey the laws of physics by staying positive if the basis function are required to fulfil the partition of unity principle.

4 Experiments: How does the 4D Spline Image model compare to the 3D model?

To test the 4D approach a simulation study with known ground truth was performed. The data used for the simulation studies is seen in Figure 1. It shows a slice in the ground truth phantom volume at phase 1 to 5. The volume consist of 2 cylinders dilating with phase to emulate the behaviour of a lung. A complete cycle has to contract from phase 5 to 1. An example of a simulated projection is shown as the thing in Figure 1. To examine the value of the method it was compared to the basic 3D iterative reconstruction with the base number of number of projections per phase being 5, 10 and 20. Each projection by design was recorded with a unique projection angle such that all the phases covers a complete rotation of 360 degrees rotation. All of the reconstruction experiments were based on running 50 iterations. Evaluation of the reconstructions were done using cross correlation, thus a perfect reconstruction should yield correlation 1. The results of this method study are shown in table 1. At a high number of projections the table indicates that a 4D model is unnecessary for reconstructing the phantom. At a lower number of projections the benefit of using a 4D spline become evident since the 3D reconstruction can deteriorate immensely while the change is comparably small in the 4D case. If we inspect the result of the experiment with 10 projections at phase

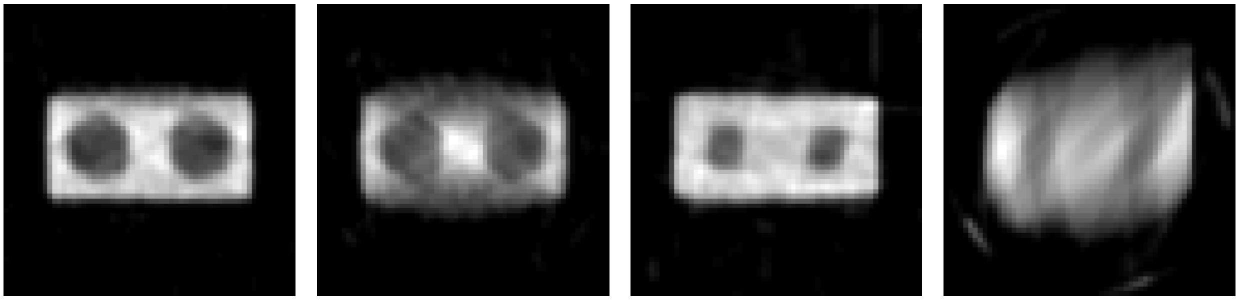

(a) 4D - (10 projs., phase 4) (b) 3D - (10 projs., phase 4) (c) 4D - (5 projs., phase 1) (d) 3D - (5 projs., phase 1)

Figure 2: Shows a slice in the reconstructed phantom volume from 2 different experiments.

4 and 5 projections at phase 1, the 4D spline model is clearly seen to benefit from being based on projection data from its nearest neighbours while the 3D reconstruction suffers from under sampling. A slice from each of these just mentioned reconstructions is shown in Figure 2. It includes the same slice reconstructed for both the 3D and 4D image model.

5 Discussion

The study performed on artificial 4D data demonstrated how fitting a 4D attenuation model from 2D projections with temporal information can lead to a better reconstruction compared to iteratively fitting a 3D model estimated from 2D projections residing at one particular temporal phase. The study comparing the 3D and 4D fitted models were especially in favour of the 4D model when the number of projections at a particular phase decreased. This type of temporal under-sampling could arise in some clinical scans.

References

[1] J. Beutel, J. M. Fitzpatrick, S. C. Horii, Y. Kim, H. L.Kundel, M. Sonka, and R. L. Metter. *Handbook of Medical Imaging, vol. 2*. SPIE-The international Society for optical engineering, 2007.

[2] L. A. Feldkamp, L. C. Davis, and J. W. Kress. Practical cone-beam algorithm. *J. Opt. Soc. Am. A*, 1(6):612–619, June 1984.

[3] R. Gordon, R. Bender, and G. T. Herman. Algebraic reconstruction techniques (art) for three-dimensional electron microscopy and x-ray photography. *Journal of Theoretical Biology*, 29(3):471 – 481, 1970.

[4] J. Hinkle, P. T. Fletcher, B. Wang, B. Salter, and S. Joshi. 4d map image reconstruction incorporating organ motion. In *IPMI '09: Proceedings of the 21st International Conference on Information Processing in Medical Imaging*, pages 676–687, Berlin, Heidelberg, 2009. Springer-Verlag.

[5] J. Nocedal. Updating quasi-newton matrices with limited storage. *MATHEMATICS OF COMPUTATIONS*, 35:773–782, July 1980.

[6] S. Rit, J. Wolthaus, M. Herk, and J.-J. Sonke. On-the-fly motion-compensated cone-beam ct using an a priori motion model. In *MICCAI '08: Proceedings of the 11th international conference on Medical Image Computing and Computer-Assisted Intervention - Part I*, pages 729–736, Berlin, Heidelberg, 2008. Springer-Verlag.

[7] J.-J. Sonke, L. Zijp, P. Remeijer, and M. van Herk. Respiratory correlated cone beam ct. *Medical Physics*, 32(4):1176–1186, 2005.

[8] R. Zeng, J. Fessler, and J. Balter. Estimating 3-d respiratory motion from orbiting views by tomographic image registration. *IEEE Transactions on Medical Imaging*, 26(2):153–163, February 2007.